Hydrol. Earth Syst. Sci. Discuss., https://doi.org/10.5194/hess-2019-121
Manuscript under review for journal Hydrol. Earth Syst. Sci.
Discussion started: 3 April 2019

Hydrology and Earth System Sciences
Open Access
Discussions

Characterization of Hillslope Hydrologic Events Using Machine Learning Algorithms

Eunhyung Lee[1] and Sanghyun Kim[1]

[1]Department of Environmental Engineering, College of Engineering, Pusan National University, Busan, South Korea

Correspondence to: Sanghyun Kim (kimsangh@pusan.ac.kr)

Key Points:

- We analyzed rainfall and soil wetness dataset with machine learning algorithms.
- Seven delineated clusters of hydrologic events represent distinct hydrological processes.
- Representative soil moisture monitoring points can be obtained using the machine learning methods.

Hydrol. Earth Syst. Sci. Discuss., https://doi.org/10.5194/hess-2019-121
Manuscript under review for journal Hydrol. Earth Syst. Sci.
Discussion started: 3 April 2019

Hydrology and Earth System Sciences
Open Access
Discussions

Abstract

Time series of soil moisture were measured at 30 points for 396 rainfall events on a steep, forested hillslope between 2007 and 2016. We then analyzed the dataset using an unsupervised machine learning algorithm to cluster the hydrologic events based on the dissimilarity distances between weighting components of a self-organizing map (SOM). Generation patterns of two primary hillslope hydrological processes, namely, vertical flow and lateral flow, at the upslope and downslope areas were responsible for the distinction of the hydrologic events. Two-dimensional spatial weighting patterns in the SOM provided explanations for the relationships between rainfall characteristics and hydrological processes at different locations and depths. High reliability in hydrologic classification was achieved for both the driest and wettest events; as assessed through k-fold cross validation using 10 years of data. Representative soil moisture monitoring points were found through temporal stability analysis of the event structure delineated from the machine learning classification. Application of a supervised machine learning algorithm provided a scheme using soil moisture for the cluster identification of hydrologic event even without rainfall data which is useful to configure hillslope hydrologic process with the least cost in data acquisition.

Keywords: rainfall, soil moisture, hillslope hydrology, temporal stability, machine learning

Hydrol. Earth Syst. Sci. Discuss., https://doi.org/10.5194/hess-2019-121
Manuscript under review for journal Hydrol. Earth Syst. Sci.
Discussion started: 3 April 2019

1 Introduction

Information on soil moisture is critical for assessing water storage, estimating the amount of runoff generated, and determining slope stability for hillslopes during rainfall (Angermann et al., 2017; Lu and Godt, 2008; Penna et al., 2011; Tromp van-Meerveld and McDonnel, 2005). Hillslope hydrological processes are affected by many factors including topographic, soil textural, and eco-hydrologic parameters (Baroni et al., 2013; Liang et al., 2011; Rodriguez-Iturbe et al., 2006; Rosenbaum et al., 2012; Wilson et al., 2004), which results in highly nonstationary and heterogeneous temporal and spatial distributions of soil moisture (Penna et al., 2009; Wilson et al., 2004). The relationship between precipitation and runoff is highly nonlinear, and the spatio-temporal variations in soil moisture, groundwater, and surface runoff are extremely difficult to predict (Ali et al., 2013; Curti et al., 2014).

Temporal stability has been widely used for selecting representative points for the characterization of soil moisture variation (Minet et al., 2013; Vachaud et al., 1985). Temporal stability depends on soil depth, soil properties, land use, surface & subsurface topography and hydrometeorological conditions (Gao and Shao, 2012; Gao et al., 2015). Both the mean and standard deviation of the relative difference had been used to evaluate the temporal stability of soil moisture (Zhao et al., 2010). High stability is an important criterion for determining the best location for the monitoring spatially averaged soil moisture of a given area (Brocca et al., 2010; Penna et al., 2013; Ran et al., 2017). The location of spatially representative soil moisture points can be also explored in the context of process-based interpretations (Lee and Kim, 2017).

Rainfall is the primary driver of rapid variations in soil moisture and subsurface flow generation (Penna et al., 2011). The response of soil moisture to rainfall events has been investigated for different topographic positions, depth profiles, and land cover conditions (Feng and Liu, 2015; He et al., 2012; Wang et al., 2013; Zhu et al., 2014). The functional relationship between rainfall events and soil moisture varies and depends on various factors such as soil texture, depth, topography, and vegetation cover (Liang et al., 2011; Bachmair et al., 2012; Kim, 2016). Various rainfall characteristics including the total amount, duration, intensity, and dry period duration also have been used to understand the soil moisture response (Alberson and Kiely, 2001; Heisler-White et al., 2008). Other studies of rainfall features have categorized rainfall events for the analysis of soil moisture variation (Lai et al., 2016; Wang et al., 2008).

The generation of distinct hillslope flow paths; vertical flows such as matrix flow and bypass flow and lateral flows along different boundaries (e.g., subsurface stormflow over bedrock and surface overland flow) can be

64 differently appeared between upslope and downslope. The functional relationship between rainfall and soil water
65 storage had been studied (Brocca et al., 2005; Castillo et al., 2003; Xie and Yang, 2013), but how the rainfall features
66 such as rainfall amount, intensity, duration and antecedent soil moisture condition influence hydrological processes
67 and their distributions at the hillslope scale had not been explored yet. Studies in hillslope hydrology had focused
68 several events to identify specific flow path (e.g., subsurface lateral flow) using intensively collected field
69 measurements for relatively short periods (Freer et al., 2004; Kim 2009; Penna et al., 2011; Wienhöfer and Zehe,
70 2013). A comprehensive approach can be explored to address the holistic behavior of hydrological processes using an
71 extended dataset. Pattern recognition capabilities of dataset have proved useful for evaluating the dissimilarity of
72 hydrologic measurements between different hydrologic events. The self-organizing map (SOM) method has been used
73 to investigate datasets representing ecosystems, animals, catchment classification, and crop evapotranspiration
74 (Adeloye et al., 2011; Farsadnia et al., 2014; Ley et al., 2011; Liu et al., 2011; Park et al., 2003). The SOM can be an
75 effective method to understand a big hydrologic data through reducing dimensionality of dataset which can provide
76 hydrologic interpretation. The highly heterogeneous and extremely nonstationary variation in soil moisture between
77 the upslope and downslope areas as well as the upper and lower soil layers of a hillslope can be analyzed by using an
78 SOM.

79 Machine learning techniques have been applied to soil moisture data from both in-situ measurements (Van
80 Arkel and Kaleita, 2014) and remote sensing applications (Ahmad et al., 2009; Prashant et al., 2013). Supervised
81 learning algorithms were used to improve predictions of subsurface flow in a hillslope (Bachmair and Weiler, 2012),
82 to downscale satellite soil moisture data (Prashant et al., 2013), and to estimate soil moisture obtained through
83 regression analysis (Ahmad et al., 2009). Identification of critical soil moisture sampling points has also being done
84 using an unsupervised learning algorithm (Van Arkel and Kaleita, 2014). Most studies involving the use of machine
85 learning algorithms for the analysis of soil moisture have focused on estimating and determining the appropriate
86 measurement locations for assessing the variations in mean soil moisture.

87 In this study, we aimed to answer the following research questions:

88 1. How can machine learning algorithms be used to understand the soil moisture response patterns at the
89 hillslope scale?

90 2. Can delineated clusters of hydrologic events be explained by different hillslope hydrological processes?

3. How can the representative soil moisture monitoring points be obtained through supervised machine learning to determine the variation of mean soil moisture, and to distinguish hydrologic events?

In this study, an alternative understanding of hillslope hydrologic behavior is explored through a long term data analysis with machine learning. Hydrologic events for the hillslope scale can be characterized through rigorous classification of a big hydrologic dataset. In particular, machine learning algorithms provide several opportunities for understanding hydrologic events through the transformation of a substantial dataset into compact clusters and for delineating the hierarchical relationship between clusters, which can be useful for exploring process-based interpretations and for obtaining an efficient monitoring network. We used a hydrologic data (throughfall and soil moisture) to analyze and characterize the highly complex relationships between antecedent soil moisture, rainfall characteristics, and soil moisture responses. An unsupervised neural network method, namely, a self-organizing map (SOM), was introduced to investigate the nonlinear interactions between various rainfall characteristics and their effects on temporal change in soil moisture, and to classify the multivariate datasets in terms of the likely flow paths in the hillslope. A supervised machine learning algorithm, namely, a C4.5 decision tree (Quinlan, 1993), was then employed to obtain optimal soil moisture points to characterize rainfall events; thus, we were able to efficiently identify the hydrologic events with less soil moisture sensor data and determine the mean soil moisture variation.

To address these research topics, we employed the following research approaches. First, we applied an SOM algorithm to datasets composed of throughfall and soil moisture distributions from upslope to downslope locations in the study area. The dataset was reclassified based on the weighting vectors of each neuron in the SOM map by using the Euclidean distances between 10 hydrologic variables from different hydrologic events.

Secondly, the nonlinear relationship between throughfall and soil moisture was evaluated by comparing the spatially weighted patterns of rainfall characteristics and soil wetness variables. The relationships between particular throughfall characteristics and soil moisture at different depths and locations were investigated, and these data were used for interpretations of hydrological processes.

Thirdly, representative sampling points of soil moisture for each distinct hydrologic classification were identified. The decision scheme made with selected soil moisture points showed the potential for using a supervised machine learning algorithm to identify hydrological processes with minimal monitoring costs.

Hydrol. Earth Syst. Sci. Discuss., https://doi.org/10.5194/hess-2019-121
Manuscript under review for journal Hydrol. Earth Syst. Sci.
Discussion started: 3 April 2019

Hydrology and Earth System Sciences
Open Access
Discussions

2 Materials and Methods

2.1 Study Area and Data Acquisition

The study hillslope (4000 m^2) is located in the Sulmachun watershed (8.5 km^2), which is a headwater of the Imjin River in northwestern South Korea (Figure 1). The study area is primarily covered by a mixture of *Polemoniales*, shrubby *Quercus*, and a coniferous canopy of *Pinus densiflora*, and the slope varies between 30° and 45°. Rainfall, streamflow, and other hydrometeorological records (e.g., temperature and relative humidity) have been collected over the last 25 years from seven hydrologic monitoring stations in this watershed (see Figure 1). Mean annual rainfall for the last two decades was approximately 1,500 mm; 70% of the total rainfall fell during the Asian monsoon season between June and August. Precipitation occurred as snowfall between December and March. Mean annual evaporation was approximately 420 mm, estimated with the eddy-covariance method by using data obtained from a flux tower (adjacent hydrologic monitoring station) located 50 m away from the study area; monthly evaporation exceeded the accumulated rainfall only in October 2010. Average daily temperature varied between −15 and 35°C. The hillslope bedrock consists of granite with extensively weathered areas. Elevations range between 200 and 260 m above sea level, and the surface slope varied between 20° and 35°. Leptosol and Cambisol (classifications from the Food and Agricultural Organization of the United Nations (FAO)) are the dominant soils of the upslope and downslope areas, respectively. Analysis of 15 soil samples (five points each for the upslope, middle slope, and downslope areas at depths of 30 cm) indicated that the predominant soil textures are sandy loam and loamy sand. The average porosities were 49% and 48% for the upslope and downslope areas, respectively. Multiple insertions of an iron pole to each grid cell (0.5 m by 0.5 m) indicated that the soil depth along the hillslope varies between 25 and 95 cm. The depth of the root zone is approximately 20 to 30 cm.

Throughfall (this was used to describe rainfall characterictics) was recorded at hourly intervals by using a rainfall gauge (Automatic Rain Gauge System, Eijkelkamp) located under the canopy. The soil moisture time series were measured using a multiplex-based time domain reflectometer (TDR; MiniTRASE, SoilMoisture, 2004) at 5 locations upslope (UP1–UP5) and 5 locations downslope (DO1–DO5) (Figure 1). At each location, three TDR sensors (waveguides) were inserted parallel to the surface at depths of 10, 30, and 60 cm into the upslope side of an installation trench. Soil moisture measurements were collected bi-hourly between 2007 and 2016. There were 396 rainfall events

144 during the study period. The rainfall event was defined by the minimum duration of a dry period as 1 day and the
145 minimum amount of throughfall as 1 mm.

146

147 2.2 Temporal Stability

148 The temporal stability method can be applied to soil moisture datasets to evaluate the temporal variability in
149 soil moisture (Vachaud et al., 1985). The normalized difference between soil moisture and mean soil moisture can be
150 expressed as

151 $$\delta_{i,j}(\%) = \frac{\theta_{i,j} - \overline{\theta_j}}{\overline{\theta_j}} \cdot 100 \quad (1)$$

152 where $\theta_{i,j}$ is the measured soil moisture, at location i and time j s, respectively, and $\overline{\theta_j}$ is the spatially averaged soil
153 moisture for time j, which can be estimated as $\overline{\theta_j} = \frac{1}{n}\sum_{i=1}^{n} \theta_{i,j}$, where n is the number of soil moisture measurements
154 for the hillslope.

155 The index of temporal stability (ITS_i) was proposed to quantify the soil moisture stability at point i (Zhao et
156 al., 2010). A high ITS_i is indicative of low temporal stability, whereas a low ITS_i is indicative of high temporal stability.
157 The value of ITS_i can be calculated as follows:

158 $$ITS_i(\%) = \sqrt{MRD_i^2 + SDRD_i^2} \cdot 100 \quad (2)$$

159 The mean relative difference (MRD_i) can be calculated as $MRD_i = \frac{1}{m}\sum_{j=1}^{m} \delta_{i,j}$, where m denotes the final
160 measurement time. The standard deviation of the relative difference ($SDRD_i$) represents the variability in the
161 normalized difference for the monitoring period, which can be calculated as follows:

162 $$SDRD_i(\%) = \sqrt{\sum_{j=1}^{m} \frac{(\delta_{i,j} - MRD_i)^2}{m-1}} \cdot 100 \quad (3)$$

163

164 2.3 Unsupervised Machine Learning Algorithm

165 The SOM is an unsupervised learning algorithm that can be useful for pattern recognition for a multivariate
166 dataset from different observations. The SOM is typically a two-dimensional (2D) grid composed of either hexagonal

Hydrol. Earth Syst. Sci. Discuss., https://doi.org/10.5194/hess-2019-121
Manuscript under review for journal Hydrol. Earth Syst. Sci.
Discussion started: 3 April 2019

or rectangular elements. In this study, we used a hexagonal lattice as the output layer because it resulted in better feature of information propagation when updating more neighborhood neurons than that of the rectangular lattice (Kohonen, 2001). Based on the recommended output dimension of $5\sqrt{r}$ (Kohonen, 2001), where r is the number of events, and the 396 total rainfall events used in this study, the array structure of the SOM was specified as a 16 × 6 matrix, which corresponded to 96 neurons, i.e., the grid cells in the SOM. Each neuron had a different weighting vector (w_{ab}), where the subscripts a and b represent address codes for the variable and node, respectively. A random number was used to initialize the weighting vectors in neurons.

For a given rainfall event, the soil moisture variation at a particular point in the hillslope depends not only on the rainfall, but also on other environmental factors such as the location, depth, and soil texture. In order to consider the relative variation (%) of water storage normalized by the antecedent moisture condition, we used the percentage of maximum soil moisture difference (Zhu et al., 2014) as an index, namely, the soil moisture difference index, to represent soil moisture variation:

$$\Delta\theta(\%) = \frac{\theta_{max}-\theta_{ant}}{\theta_{ant}} \cdot 100 \quad (4)$$

where θ_{max} is the maximum soil moisture during a rainfall event and the subsequent period (≤ 4 h), and θ_{ant} is the soil moisture measurement before the rainfall event (2 hours).

Once the dataset is populated with the throughfall characteristics and soil moisture data, the SOM map (Kohonen, 2001) can be obtained. In this study, throughfall duration, total throughfall amount, and mean throughfall intensity were used as the rainfall characteristics, and the antecedent moisture content, soil moisture difference for 5 locations upslope at depths of 10, 30, and 60 cm, and soil moisture difference for 5 locations downslope at depths of 10, 30, and 60 cm were used for the soil moisture data (Figure 1). Because each variable had a different range, we applied a natural logarithm transformation out of several transformations such as Box-Cox transformations with different parameters to the dataset standardize the variables, which centralize the means of all variables into zero.

The SOM maps were established to each variables and the distance between the input vector and weighting vector can be calculated as follows:

$$d_b = \sqrt{\sum_{a=1}^{v}(w_{a,b} - x_a)^2} \quad (5)$$

where v is the number of variables.

Hydrol. Earth Syst. Sci. Discuss., https://doi.org/10.5194/hess-2019-121
Manuscript under review for journal Hydrol. Earth Syst. Sci.
Discussion started: 3 April 2019

193 The winner neuron can be identified as the neuron with the minimum value of d_b indicating the best fitness
194 to characteristics of each rainfall event among every neruons in SOM map. If the winner neuron is chosen, the
195 weighting vector should be re-evaluated by using the Eq. for the renewal weighting vector as follows:

$$\Delta w_{a,b} = \begin{Bmatrix} \alpha(x_a - w_{a,b}) & b = b^* \\ 0 & b \neq b^* \end{Bmatrix}$$

196 $$w_{a,b}^{new} = w_{a,b}^{old} + \Delta w_{a,b} \quad (6)$$

197 where α (= 0.5) is an acceleration coefficient and b^* is the winner neuron. Neurons adjacent to the winner neuron are
198 also updated through the application of Eq. (6). Both the radius of neighboring neurons and acceleration coefficient
199 decreased (from 16 to 1) linearly as the iterations approached the maximum iteration.

200 After finishing the work with the updating algorithm, all neurons in the SOM maps had fitted weighting
201 vectors to the multiple datasets of this study. The probability density function of each input variable leading to
202 selection of each specific SOM node can then be inferred from the weighting vector. The input variables in each
203 neuron can be displayed in the form of a spatial pattern in the SOM maps. They have many kinds of spatial patterns,
204 which correspond to the number of variables. Additionally, the displays for one variable and many variables are called
205 the “component plane” and “component planes,” respectively. The nonlinear relationship between variable was
206 identified through visual comparison between the spatially distributed weightings in each component plane (Adeloye
207 et al., 2011; Farsadnia et al., 2014; López García and Machón González, 2004; Park et al., 2003).

208

209 2.4 Clustering

210 Clusters within the dataset can be delineated by applying the dendrogram classification method and by
211 evaluating the dissimilarity between the weighting vectors (Montero and Vilar, 2014). In this study, we used a
212 hierarchical method because the resulting dendrogram structure provided better representation for the relationships
213 between clusters than the results obtained by using non-hierarchical methods. The hierarchical method forms clusters
214 by binding datasets with shorter distances between them. The Euclidean distance was employed to evaluate the
215 dissimilarity because it is suitable for shape-based comparisons between soil moisture series collected at the same
216 time (Iglesias and Kastner, 2013). This method also used to identify clusters of soil moisture data (Van Arkel and

Hydrol. Earth Syst. Sci. Discuss., https://doi.org/10.5194/hess-2019-121
Manuscript under review for journal Hydrol. Earth Syst. Sci.
Discussion started: 3 April 2019

Kaleita, 2014). The Euclidean distance between two weighting vectors in the neurons (b_1 and b_2) can be expressed as follows:

$$d_{b_1 b_2} = [\sum_{a=1}^{v}(w_{a,b_1} - w_{a,b_2})^2]^{0.5} \quad (7)$$

The relationship that has the shortest distance between neurons is assigned to the first cluster, and weighting vectors of the first cluster can be expressed as

$$\mu_{c_1,a} = \frac{n_{b_1}\mu_{b_1} + n_{b_2}\mu_{b_2}}{n_{b_1} + n_{b_2}} \quad (8)$$

where μ_{b_1} and μ_{b_2} are the variable weighting vectors in the neurons (b_1 and b_2), respectively; n_{b_1} and n_{b_2} are set to 1 in this relationship, but these values are set to the numbers of components during the comparisons of clusters. Additionally, we used Ward's method to evaluate the dissimilarity between two weighting vectors of each neuron, and between each cluster, i.e., this was the chosen algorithm in our hierarchical clustering method (Ward, 1963). When the dissimilarity between two clusters (c_1 and c_2) is calculated, the distance between the clusters can be expressed as

$$d_{cluster} = \sum_{a=1}^{v} \frac{\|\mu_{a,c_1} - \mu_{a,c_2}\|^2}{\frac{1}{n_{c_1}} + \frac{1}{n_{c_2}}} \quad (9)$$

where μ_{a,c_1} and μ_{a,c_2} are the averages of clusters c_1 and c_2, respectively, and n_{c_1} and n_{c_2} are the numbers of components for clusters c_1 and c_2, respectively. A dendrogram can be constructed based on the resulting $d_{cluster}$, and the upper part from a designated horizontal line can be recognized as the structure of the final clusters.

2.5 Water Storage Evaluation

The water storage after a rainfall event can provide a better understanding about what flow paths or combined processes contribute to the redistribution of soil water along the hillslope. The water storage can be evaluated following a multiplication step for the corresponding soil depth (i.e., 200 mm for soil moisture at the depths of 10 and 30 cm, and 300 mm for soil moisture at the depth of 60 cm) related to the maximum difference of soil moisture between prior and post rainfall conditions. The distribution of water storage in depth profile and hillslope location (upslope or downslope) indicate distinct hydrological processes along the hillslope. The collected throughfall data can be used for the effective rainfall while neglecting evaporation for the short period of analysis.

Hydrol. Earth Syst. Sci. Discuss., https://doi.org/10.5194/hess-2019-121
Manuscript under review for journal Hydrol. Earth Syst. Sci.
Discussion started: 3 April 2019

241 2.6 Supervised Machine Learning Algorithm

242 One of the most reliable supervised learning algorithms is the C4.5 algorithm (Quinlan, 1993), which can be
243 used for regression or classification of multivariate data. The C4.5 algorithm is based on the selection of the attribute
244 that yields the maximum information gain from data subsets. The information gain can be calculated as follows:

245 $$H(X) = \sum_{x \in X} p(x) log_2(\frac{1}{p(x)}) \quad (10)$$

246 where $H(X)$ is the entropy of all clusters, which is a measure of uncertainty, $p(x)$ is the proportion of element numbers
247 in each cluster, and X is the number of clusters. In other words, the entrophy for cluster delineations from SOM can
248 be obtained from equation (10).

249 In order to obtain the threshold of soil moisture difference index, the information gain is introduced. The
250 higher information gain represents the better threshold for cluster identification. The information is a measure of the
251 difference in prior and post entropy for the set, which is split on the attribute A as

252 $$IG(A, X) = H(X) - \sum_{t \in T} p(t) H(t) \quad (11)$$

253 where $IG(A, X)$ is the information gain from the classification of attribute A (i.e., A is the criteria for the specific soil
254 moisture difference at a designated point), T is either greater than A or less than A, and *t* is a subset of T. The term in
255 equation (11), $p(t)$, is composed of two conjugate probabilities; the events have smaller soil moisture difference index
256 then the threshold divided by total events and the events have greater soil moisture difference index then the threshold
257 divided by total events.

258 The C4.5 algorithm can be used to identify a specific soil moisture point that can be used to classify a
259 designated cluster by calculating the entropy. Thresholds for all soil moisture monitoring point are evaluated and the
260 one having highest information gain is selected as a classifier of decision tree and the identical procedure is repeated
261 to obtain the C4.5 decision tree of soil moisture difference indices. Depending on the soil moisture characteristics for
262 several points, the main feature of the hydrologic system can be identified. A decision tree, namely, a sequential
263 structure of soil moisture criteria, can be developed for the specific locations of soil moisture with the maximum
264 information gain. In other words, the soil moisture variation of the selected measurement points can be used to
265 delineate identical clusters obtained by the dendrogram classification method.

266

Hydrol. Earth Syst. Sci. Discuss., https://doi.org/10.5194/hess-2019-121
Manuscript under review for journal Hydrol. Earth Syst. Sci.
Discussion started: 3 April 2019

3 Results

3.1 Representative Point for Soil Moisture Measurement

The ITS of soil moisture was estimated for 10 locations (Figure 1(b)) at three soil depths (10, 30, and 60 cm) to determine a representative point for analyzing the soil moisture variation for rainfall events. The ITSs for soil moisture measurements at 30 points showed that both the location and depth affected the stability of soil moisture (Figure 2). The ITS tended to be higherr at deeper depths because of the impact of hydrometeorological drivers (e.g., rainfall and evaporation) and intermittent generation of subsurface storm flow at deeper depths, which corresponds to the results from a previous study (Lee and Kim, 2017). Location UP5 had the lowest ITS of the 10 locations, and thus, it represents the most temporally stable soil moisture (at all depths). UP3-10 had the lowest ITS_i of all 30 points; specifically, the value was 0.13. Figure 3 shows the soil moisture at both the most temporally stable point (UP3-10) and the least temporally stable point (DO5-30) for representing the average soil moistures of all points. As shown in Figure 3, RMSEs (root mean square errors) were 2.22% for UP3-10 and 8.72% for DO5-30. The representative point, which had the lowest ITS, was correlated more with the average soil moisture than any other point. Therefore, the soil moisture measurement for UP3-10 was adopted as the representative soil moisture before the event for the SOM analysis.

3.2 Composition and Clustering of the SOM

With the application of the SOM method, the dataset of hydrologic measurements (396 × 10) was transformed through 96 neurons and output in terms of a matrix (16 × 6) through the iterative application of Eqs. (5) and (6). In other words, 10 hydrologic variables from 396 events were expressed compactly in the SOM.

Dissimilarity in terms of the Euclidean distance between output neurons was then used to construct the dendrogram. Many alternatives exist to number of clusters depending on the complexity of the dendrogram structure. In this study, seven clusters was selected based on a heuristic approach aiming to achieve a hydrologically meaningful classification of events and parsimonious clustering. The relation to notable hydrological processes such as lateral flow or vertical preferential flow and the redundancy check in cluster number were important factors in the heuristic approach. Figure 4(a) shows the resulting dendrogram for the seven clusters. The structure of the dendrogram shows

293 the relationships between groups of clusters and between individual clusters. For example, the relationship between
294 clusters 5 and 6 had a lower hierarchy than that of clusters 3 and 4. Figure 4(b) presents the output SOM (16 × 6)
295 delineated from the dendrogram analysis, which is a structural array identical to the delineated dendrogram with
296 neurons for each cluster. The spatial distributions between other clusters and corresponding numbers of neurons
297 indicate the areal portion of each cluster from all clusters and its connection with adjacent clusters. Table 1 presents
298 the average vector components (e.g., duration of rainfall (DUR), amount of throughfall (AMO), intensity of
299 throughfall (INT), antecedent soil moisture (ASM) in volumetric %, UP10, UP30, UP60; average of the soil moisture
300 difference indices (Δθ) in five upslope locations at a depth of 10 cm, 30 cm, and 60 cm, respectively, DO10, DO30,
301 and DO60; average of the soil moisture difference indices (Δθ) in five downslope locations at depths of 10 cm, 30 cm,
302 and 60 cm, respectively) for the seven clusters shown in Figures 4(a) and 4(b).

303 As shown in Figure 4(b), clusters 1 and 2 were located in the upper part of the SOM. Table 1 indicates that
304 the rainfall characteristics of clusters 1 and 2, such as DUR, AMO, and INT, were relatively low and that the antecedent
305 soil moisture was similar to the mean ASM for all clusters (Figure 5). The average soil moisture difference indices
306 were less than 5% for cluster 1 because the low throughfall amount and intensity resulted in a limited increase in soil
307 water storage, and the loss due to evaporation offset a substantial proportion of the precipitation (Albertson and Kiely,
308 2001; Ramirez et al., 2007). Cluster 1 was most similar to cluster 2 but had higher throughfall amounts and intensities
309 (see Figure 4(a)). The intermediate part of the SOM (Figure 4(b)) included clusters 3 and 4, which had higher
310 throughfall durations, amounts, and intensities than clusters 1 and 2. The soil moisture difference indices for clusters
311 3 and 4 were higher than those for clusters 1 and 2. The higher throughfall durations and amounts for cluster 4 were
312 associated with higher soil moisture difference indices for cluster 4, but the lower throughfall for cluster 3 resulted in
313 smaller soil moisture difference indices (Table 1). One notable feature of clusters 3 and 4 was the increasing trend of
314 soil moisture difference indices with depth (DO60 > DO30) for the downslope area, whereas those of clusters 1 and 2
315 showed decreased soil moisture difference indices with depth (DO30 > DO60) (Table 1).

316 The events showing similarity with larger soil moisture difference index, namely, significant events, in the
317 SOM were in clusters 5, 6, and 7, as shown in Figure 4(b). The pattern of soil moisture difference indices for cluster
318 5 was indicative of vertical infiltration upslope and strong lateral flow downslope (Table 1 and Figure 4), which were
319 distinct from cluster 6. The soil moisture difference indices for cluster 5 were larger than those of cluster 6, except for
320 UP60 (9.6%), even with the lower throughfall duration, amount, intensity, and antecedent soil moisture than those for

cluster 6. Both rainfall characteristics and soil moisture difference indices for cluster 7 were significantly higher than those for all other clusters. Many of the measurement points in cluster 7 were saturated throughout rainfall events, and the DO10 value of cluster 7 was 192.6% (48.2% in terms of volumetric soil moisture), which indicates that overland flow occurred was likely at the downslope points.

3.3 Water Storage Analysis

We selected a rainfall event from each of the seven clusters that showed the distinct characteristics of hydrological processes associated with each cluster for the analysis. The water storage distribution analysis for seven rainfall events is presented in Table 2. Water storage analysis for clusters 1 and 2 showed that negligible changes in water storage occurred for both the upslope and downslope areas, and the main difference between cluster 1 and cluster 2 was whether the rainfall affected the soil moisture difference index (%) at a depth of 60 cm in the upslope area (Table 2). Rainfall impacts to clusters 3 and 4 were classified into the intermediate category because both clusters introduced meaningful storage change (mm) and soil moisture difference index (%) in the deepest depths of the downslope area (60 cm) indicative of the generation of subsurface lateral flow. Significant changes in water storage (>40 mm) were found for clusters 5, 6, and 7 regardless of the amount of throughfall. The main difference between clusters 5 and 6 was whether the vertical preferential flow affected the 60 cm soil layer in the upslope area, which depended on the antecedent soil moisture. Cluster 7 was mainly associated with very high amounts of rainfall, and subsurface lateral flow was generated in both the upslope and downslope areas; additionally, exceptionally large changes in water storage (>116 mm) occurred in the downslope area.

3.4 Component Planes of Each Variable

The component planes of 10 variables and their visual comparisons can provide a better understanding of the nonlinear relationships between the 10 hydrological variables. Figures 5(a)–5(j) show the vector component weightings of the 10 variables. Both the spatial distributions and the scales of weightings (scale bar) in Figure 5 represent the characteristics of impacts (rainfall characteristics and antecedent soil moisture) and consequences (soil moisture difference). As shown in Figures 5(a), 5(f) and 5(g), higher weightings for the throughfall amount,

347 throughfall duration, and throughfall intensity were located in the lower-right part of the SOM map. The SOM map
348 for antecedent soil moisture showed dry conditions in the lower-left part and wet conditions in the lower-central
349 portion (Figure 5(b)). Visual comparison between rainfall features and antecedent soil moisture revealed that the
350 correlation between throughfall and antecedent soil moisture was negligible. Therefore, the periods between the
351 rainfall events were long enough on average that the influence of previous rainfall events on soil moisture variation
352 was negligible.

353 Figure 5(c) shows the weightings of soil moisture difference indices upslope at a depth of 10 cm, which is
354 the soil layer influenced by direct precipitation with negligible impacts from the upslope area. The combined
355 throughfall amount weightings (Figure 5(a)) and throughfall intensity weightings (Figure 5(f)) appeared similar to the
356 weightings in Figure 5(c). Similar weighting distributions were observed for the upslope area at depths of 30 cm and
357 60 cm (Figures 5(d) and 5(e)) with degreasing trend in deeper depth, which corresponds to cluster 5. Weightings of
358 soil moisture difference indices for the downslope area (Figures 5(h)–5(j)) showed less variation in the horizontal
359 direction in the lower part than those for the upslope area indicating the behaviors of clusters 5, 6, and 7 are similar in
360 downslope. This means that the soil moisture variations for the downslope area were less correlated to rainfall
361 characteristics than those for the upslope area. The soil moisture difference index map for the downslope area at a
362 depth of 10 cm (Figure 5(h)) was correlated only to the throughfall intensity (Figure 5(f)). The soil moisture difference
363 indices at depths of 30 cm and 60 cm (Figures 5(i) and 5(j)) showed distributions that were less horizontally skewed
364 in terms of the weighting than those for the depth of 10 cm (Figure 5(h)). The impact of rainfall and antecedent soil
365 moisture appeared to be dampened at greater depths downslope. No notable correlation was found between ASM
366 (Figure 5(b)) and soil moisture difference indices.

367

368 3.5 Validation of the SOM Classification

369 The reliability of the SOM application for hydrologic events was also evaluated through comparison of the
370 SOM made from the complete dataset with those from partial datasets (k-cross validation, k = 10 years). Multiple
371 SOMs were made with datasets missing events in 2016, 2015, ..., and 2007, which resulted in 10 SOMs from
372 incomplete datasets for a 10-year period. SOMs from partial datasets had identical dendrogram structures to that of
373 the complete dataset, which resulted into seven clusters shown in Figure 4. The numbers of neurons for each of the

374 seven clusters cannot be identical between the 10 SOMs. To evaluate the robustness of the SOM characterization,
375 different missing events for each of the 10 incomplete datasets were projected to each of the corresponding 10 SOMs
376 made from partial datasets. In other words, unused datasets for each of the 10 training datasets were used to reclassify
377 neurons and cluster numbers by evaluating the Euclidean distances between the weighting vectors. Figure 6 presents
378 the matrix expression between the event projections for the SOM shown in Figure 4(b) and the sum of event
379 projections from the 10 SOMs made from partial datasets. For clusters 1, 5, and 7 in the matrix (Figure 6), there was
380 more than 90% agreement in event numbers between the complete SOM and the other partial classifications, whereas
381 cluster 2 resulted in 49% agreement in terms of the classification, which was mainly related to misidentifications
382 between cluster 2 and cluster 1. The number of agreements from k-cross validation was 317 out of 396 hydrologic
383 events in 10 years.

384

385 3.6 Supervised Machine Learning for Soil Moisture Representative Points

386 The stability of soil moisture has been widely assessed to obtain representative points for studying the variation
387 in mean soil moisture (Brocca et al., 2010; Ran et al., 2017; Vachaud et al., 1985). Unlike in the ITS analysis, the soil
388 moisture monitoring points for effective discrimination between different clusters should be sensitive to rainfall events,
389 and also effectively address hydrological processes such as infiltration and soil water redistribution along the hillside.
390 A decision-making process for cluster identification can be expressed in terms of a decision tree. Thus, the supervised
391 machine learning algorithm was applied to construct a C4.5 decision tree (Quinlan, 1993).

392 As shown in Figure 7, the C4.5 decision tree consisted of soil measurement points in the upslope (UP3-10,
393 UP5-10, UP4-60, UP5-60) and downslope (DO3-10, DO4-10, DO5-10, DO2-60) areas. From the delineated decision
394 tree (Figure 7), the point at DO2-60 provided the greatest information gain from all points because soil moisture
395 difference index at this point determined the distinctions between clusters 6 and 7, clusters 4 and 5, clusters 1 and 2,
396 and clusters 4 and 5. A point at UP5-60 contributed to the discrimination between cluster 3, cluster 4, and cluster 5
397 from cluster 6 and cluster 7, and a point at DO5-10 was used to distinguish between cluster 2 and cluster 3. Furthermore,
398 point UP4-60 was important for determining the difference between cluster 1 and cluster 2, while point DO3-10 was
399 important for determining the difference between cluster 3 and cluster 4.

400

Hydrol. Earth Syst. Sci. Discuss., https://doi.org/10.5194/hess-2019-121
Manuscript under review for journal Hydrol. Earth Syst. Sci.
Discussion started: 3 April 2019

401 **4 Discussion**

402 4.1 Hydrological Processes

403 Application of an unsupervised machine learning algorithm, namely, SOM, to the dataset provided an
404 integrated assessment to evaluate and characterize hydrologic events. Then, soil moisture recharge could be inferred
405 based on the rainfall characteristics and antecedent moisture content. In other words, the recharge patterns of water
406 storage for soil layers of the hillslope were characterized by several distinct clusters. The hydrologic events were
407 classified into three distinct categories, which depend on the generation subsurface lateral flow in downslope
408 (discussing in the following section), and seven further refined clusters as follows: insignificant events for clusters 1
409 and 2, intermediate events for clusters 3 and 4, and significant events for clusters 5, 6, and 7. Further classification of
410 significant events indicated that the effects of antecedent moisture conditions and throughfall amounts were critical to
411 delineating cluster 5 and cluster 7. The generation of lateral flow in deep soil layers of the downslope area was
412 considered to be the threshold feature between the insignificant and intermediate events; the primary difference
413 between the intermediate events and significant events was the substantial development of interface flow between
414 bedrock and soil layer in the downslope area (see Figure 8(c)).

415 As illustrated in Table 2, the distinct distribution of soil water storage can be explained by the different
416 combinations and degrees of hydrological processes (vertical flow, subsurface lateral flow, and preferential vertical
417 flow) for each cluster. The comparison between cluster 5 and clusters 4 and 6 indicated that there was strong
418 nonlinearity in the generation of hydrological processes (stronger lateral subsurface flow in the downslope area for
419 the events of cluster 5 even with small throughfall and less antecedent soil moisture than those for clusters 4 and 6).
420 This means that even though throughfall and antecedent soil moisture are important in determining hydrological
421 processes for each cluster, the generation of different hydrological processes cannot be completely explained by these
422 factors alone and the nonlinearity of hydrological responses needs to be explored.

423 The hillslope hydrological flow path was characterized through the comparison of component planes between
424 UP10 and UP30 or UP60, and other combinations of soil moisture component planes, such as those of DO10 and
425 DO30 or DO60. The exclusive vertical flow impact could be identified based on relationships between the component
426 plane for UP10 and those for UP30 or UP60 (Figures 5(c), 5(d), 5(e)) because there was small upslope contributing
427 areas or topographic wetness indices (Figure 1) in upslope locations (Beven and Kirkby, 1979). The high weightings

428 of 10 cm for the upslope area were distributed in two parts of SOM, namely, the lower-left and lower-right (Figure
429 5(c)), but those of deeper depths for the upslope area were found only on the lower-right part of SOM (see Figures
430 5(d) and 5(e)). Weightings in UP10 were associated with the throughfall amount and throughfall intensity, but those
431 for UP30 and UP60 were correlated only to the throughfall amount. A consistent pattern of weighting was found
432 between UP30 and UP60 compared to UP10, which was attributed to the effect of vertical infiltration. Furthermore,
433 the higher weightings tended to decrease as depth increased in the upslope area because the effect of vertical infiltration
434 was smaller at greater depths (Li et al., 2013). The relationships between the component plane of DO10 and those of
435 DO30 and DO60 differed (Figures 5(h)–5(j)). Even though high weightings in the middle-left part for DO10 partially
436 decreased in the component planes for DO30 and DO60, high weightings in the lower-left corner in Figure 5(h)
437 remained in Figures 5(i) and 5(j). The spatial weighting patterns of soil moisture at downslope points (Figures 5(i)
438 and 5(j)) did not show any notable correlations to those of upslope soil moisture at identical depth and rainfall
439 characteristics. This means that the flowpath in the downslope area cannot be completely explained by vertical flow.
440 Furthermore, the component plane in Figure 5(h) different from that of Figure 5(c), which means that the soil moisture
441 at a depth of 10 cm in the downslope area could have been also affected by the upslope contributing area.

442 The weighting ranges (scale bars in Figure 5) of the 10 and 60 cm depths (Figures 5(h) and 5(j)) were greater
443 than that of the 30 cm depth (Figure 5(i)). This may indicate that the lateral flow along boundaries (subsurface and
444 surface) was stronger than that at intermediate depths (Table 1). Cluster 6 and cluster 5 were located in the lower part
445 of the SOM map, as shown in Figure 4(b). As illustrated in Table 1, cluster 6 had higher amounts, durations, and
446 intensities of throughfall than cluster 5, and antecedent soil moisture for clusters 6 and 5 were the highest and lowest,
447 respectively, among all clusters. The soil moisture difference indices for cluster 6 were similar or greater than 50% at
448 all locations except DO30 (32.1%) (Table 1), which indicates that downslope lateral flow tended to be generated
449 through boundaries either along the surfaces or bedrock (Kim, 2009). Furthermore, rainfall and antecedent soil
450 moisture were substantially higher for cluster 6 than for cluster 5, and the soil moisture difference indices in cluster 6
451 were relatively more uniform for all points than those for cluster 5 (Table 1). This may be explained by the
452 development of preferential pipe flow, which is more common at greater depths in wetter conditions (Lai et al., 2016;
453 Uchida et al., 2001; Wienhöfer and Zehe, 2013). Low variation in UP60 for cluster 5 indicated that low antecedent
454 moisture conditions limited active lateral flow into the downslope area. Extreme events were mainly associated with
455 cluster 7, as illustrated in Table 1. Lateral flow likely occurred in both in the upslope and in the downslope areas for

456 cluster 7. In particular, Figures 8(b) and 8(c) show statistics for volumetric soil moisture for cluster 7 that were
457 indicative of the substantial development of saturation. As shown in Figures 5(e)–5(j), the soil moisture changes both
458 UP30 and DO30 were lower than UP10 or UP60 and DO10 or DO60, respectively. Effective drainage during extreme
459 events seemed to be strongly associated with lateral flow generation along the two boundaries in the soil media (i.e.,
460 surface and bedrock) (Freer et al., 2004; Haga et al., 2001; Kim, 2009). The impact of extreme rainfall conditions
461 dominated over other controls (e.g., land cover and topography) in terms of hillslope runoff generation (Feng and Liu,
462 2015).

463

464 4.2 Reliability in Hydrologic Event Classification

465 The contribution of each vector component to the SOM classification shown in Figure 4(b) was analyzed
466 through the distribution of statistical characteristics for each cluster, as shown in Figures 8(a)–8(c). As shown in Figure
467 8(a), the impact of ASM on the soil moisture classification was distinctive for clusters 6, 4, and 7. Even though cluster
468 5 and cluster 7 were adjacent to each other in the dendrogram structure, the ASM values for the two clusters were
469 completely different, which indicates that ASM could not have been the dominant factor for soil moisture incremental
470 changes during extreme events. Box plots of cluster 5 in relation to the throughfall duration and throughfall amount
471 were also substantially different from those of adjacent clusters such as cluster 6 and cluster 7 (see Figure 8(a)). Box
472 plots of volumetric soil moisture (VSM) by cluster generally showed increasing distributions from cluster 1 to cluster
473 7 in terms of both the mean values and variance, except for cluster 5, both in the upslope and downslope areas (Figures
474 8(b) and 8(c)). In order to test the reliability of the SOM classification, we used the k-cross validation technique for
475 10 different datasets in 10 years. Depending on the characteristics of rainfall events each year, the degree of agreement
476 of the SOM projections between the complete dataset and the partial datasets differed. A comprehensive evaluation
477 of the SOM predictability was performed through comparison between the event projections of the complete dataset
478 SOM and the summation of the projections of the 10 partial SOMs (Figure 6). All disagreement was due to missed
479 recognition between adjacent clusters (Figure 4(b)) in the SOMs from partial datasets, as shown in Figure 6. Even
480 though the cluster identification of partial dataset SOMs between adjacent clusters did not always perfectly match that
481 of the complete dataset, the predictability of extreme events was high and stable. Actually, the degree of agreement

for three categories was 92.9%. This demonstrates the reliability of the SOM for the characterization of hydrologic events of big data.

4.3 Temporal Stability and Representative Point

Considering the importance of determining the representative point for soil moisture monitoring, the classification of hydrologic events can be approached in terms of the temporal stability of soil moisture (Minet et al., 2013; Penna et al., 2013; Vachaud et al., 1985). A representative point can be also designated for all clusters through ITS analysis (Table 3). The selected points shown in Table 3 were the most temporally stable points for each cluster. The representative point for clusters 1, 2, and 5 was UP3-10 for all events, but clusters 3, 4, 6, and 7 yielded a different point (DO3-10) as the representative point. The differences in mean soil moistures and distinct hydrological processes (generation of vertical flow and lateral flow in the upslope area) throughout hydrologic events between clusters 1, 2, 5 and clusters 3, 4, 6, 7 seemed to be responsible for these two different representative points. The statistics were also different between the two representative points. The R^2 and RMSE values were evaluated between the averages of the soil moisture time series and those of a representative point in each cluster. As illustrated in Table 3, DO3-10 provided a higher R^2 than UP3-10 for clusters 3 and 4, but the RMSEs for UP3-10 were lower than those for UP3-10 for clusters 3 and 4, and the opposite was found for cluster 7. The R^2 values were identical between UP3-10 and DO3-10, DO3-10 provided lower RMSEs than UP3-10 for cluster 6. The results shown in Table 3 indicate that the two points (UP3-10 and DO3-10) can be used as representative points for the seven clusters.

The representative point for soil moisture monitoring can differ depending on the soil, depth, topography, and vegetation (Bachmair et al., 2012; Baroni et al., 2013; Gao et al., 2015; Zhu et al., 2014). Furthermore, temporal stability can be sensitive to the temporal distribution of rainfall (Penna et al., 2013). We classified 396 hydrologic events into seven clusters, and the temporal stability analysis for each cluster shown in Figure 4(a) resulted in only two points for stable variations in soil moisture. This effectiveness of representative points was partially related to the fact that the soil moisture stability analysis was performed under similar hydrologic conditions based on the identified hydrological processes shown in Table 3. The spatial and profile distributions of vertical flows and lateral flows can be comprehensively characterized through 7 clusters noted in Table 3. In other words, the soil moisture monitoring in

508 2 representative points (one in upslope and the other in downslope) provides a holistic configuration of flow paths as
509 well as the evaluation of mean soil moisture variation in the study area.

510

511 4.4 Representative Points for Cluster Identification

512 On the basis of further analysis in regard to the hydrological processes shown in Table 3, a compact set of soil
513 moisture monitoring points was selected and used to identify the seven clusters (Figure 7). As shown in Figure 7,
514 whether soil moisture difference index at DO2-60 was less than 9.2 or not was the first criterion prior to moving to
515 the next step such as determining whether the soil moisture difference index at UP5-10 was less than 5.2 or that of
516 UP5-60 was less than 16.4. One or two more steps further lead to the identification of the clusters (Figure 7).

517 Unlike in the ITS analysis, the monitoring point for the effective distinction between different clusters should
518 be sensitive to rainfall events. Including the two representative points (UP3-10 and DO3-10) for the upslope and
519 downslope areas selected from the ITS analysis, eight points were used in the C4.5 decision tree (Figure 7). The soil
520 moisture points in the C4.5 decision tree did not include any measurement point at a depth of 30 cm. This indicated
521 that the important hydrological process (lateral flow) for event distinction was mainly generated at either surface or
522 bedrock boundaries.

523 The hydrological processes indicated in Table 3 can be expressed in terms of a decision tree (Figure 9). A
524 substantial similarity was found between Figures 7 and 9 in terms of the orders of clusters between the two decision
525 trees. One or multiple diverging branches of the soil moisture difference index decision tree (Figure 7) corresponded
526 to one of the diverging branches of the decision tree for hydrological processes (Figure 9). This was because the soil
527 moisture response, whether it was greater than or less than the threshold soil moisture difference index (Figure 7), was
528 the combined result from multiple hydrological processes acting at the corresponding point.

529 The comparison between Figures 7 and 9 indicated that soil moisture difference index for DO2-60 could be
530 used to determine whether hydrologic events were significant or “other” (insignificant or intermediate) events, as well
531 as the degree of downslope hydrological processes for clusters 5, 6, and 7. The soil moisture difference index at point
532 UP5-60 was useful in identifying generations of vertical flow and lateral flow in the upslope area. The point DO5-10
533 contributed to determinations of the degree of vertical flow in the upslope area and differences in the rainfall categories

between insignificant and significant events. The existence of vertical flow in the upslope area was detected in the soil moisture difference index at UP4-60.

Even though the decision tree in Figure 7 provided an optimum monitoring set for cluster identification, the accuracy of cluster identification was less than 100%. This was due in part to our use of partial data (26%) to predict the behavior of the total dataset. The other possible explanation seemed to be related to the underlying stationary assumption of the hydrologic system for the study period (10 years). The difference in canopy activity over 10 years and the generation of catastrophic rainfall events (e.g., 145 mm in 2 hours on 27 July 2011) could have partially changed the redistribution mechanisms of soil moisture along the study area. The accuracy of the delineated decision tree (Figure 7) in identifying the seven clusters was 82 % and that of the rainfall category classification (insignificant, intermediate and significant) was 95 %. However, eight soil moisture monitoring points even without rainfall and antecedent soil moisture presented in Figure 7 demonstrated a reliable capacity for making distinctions among clusters constructed from the total dataset (rainfall characteristics, antecedent moisture, and 30 points of soil moisture difference index for 396 events) and the representative points of mean soil moisture variation in both the upslope and downslope areas. In other words, the capability of dimensionality reduction of the machine learning algorithm is useful not only in the data grouping of similar behavior with hydrologic interpretation but also in the delineating of the minimum monitoring points for the cluster identification, which can be useful to substantially reduce the cost of network maintenance.

5 Conclusions

Rainfall characteristics and the responses of soil moisture at the hillslope scale were explored through the application of machine learning algorithm to a big dataset of hydrologic responses. Hydrologic events were characterized through the application of an unsupervised learning algorithm to a soil moisture dataset collected over 10 years from a steep hillside. Based on a delineated dendrogram, classification of neurons into seven clusters and three primary event types provided meaningful interpretations to understand the hydrologic events. The upslope and downslope spatial patterns of hillslope hydrological processes, vertical flow, and lateral flow were responsible for the distinctions between the event clusters. The nonlinear relations between hydrologic variables were expressed effectively in 2D SOM presentations of variables. Comprehensive tests of the SOMs with 10 partial datasets and

projections of missing datasets revealed the robustness of the application of the SOM for the classification and prediction of extreme hydrologic events. Water storage analysis for each event from the seven clusters suggest that different combinations and contributions of vertical flow, subsurface lateral flow, and preferential flow determined the particular hydrological process dominant for each cluster. Temporal stability analysis of soil moisture time series provided efficient representative points for all delineated clusters. The soil moisture decision tree obtained from the application of a supervised learning algorithm effectively identified the clusters of hydrologic events even without abundant rainfall data and antecedent soil moisture data. The application of learning machine algorithms was useful not only to understand soil moisture variation patterns within clustered events, but also to identify the optimal monitoring locations for the mean soil moisture variation and different generations of vertical flow and lateral flow in upslope and downslope. The approach developed in this study should be applicable to other hydrological systems having sufficient data with connectivity in processes between variables.

Code and Data Availability

Code and data will be available through repository https://www.re3data.org/ when paper is accepted.

Author contribution

Enhyung Lee and Sanghyun Kim and several former graduate students had collected data for the study area. Eunhyung Lee developed model code and performed simulation. Sanghyun Kim prepared manuscript with contribution from Ennhyung Lee.

Competing interests

The authors declare that they have no conflict of interest

Acknowledgments

This study was financially supported by the Basic Research Program (2016R1D1A1B02008137) of the Korea Research Foundation of the Republic of Korea.

References

Adeloye, A. J., Rustum, R., and Kariyama, I.D.: Kohonen self-organizing map estimator for the reference crop evapotranspiration, Water Resour. Res., 47(8), https://doi.org/10.1029/2011WR010690, 2011.

Ahmad, S., Kalra, A., and Stephen, H.: Estimating soil moisture using remote sensing data: machine learning approach, Adv. Wat. Resour., 33, https://https://doi.org/org/10.1016/j.advwatres.2009.10.008, 2010.

596 Albertson, J. D., and Kiely, G.: On the structure of soil moisture time series in the context of land surface models, J.
597 Hydrol., 243, 101-119, https://doi.org/10.1016/S0022-1694(00)00405-4, 2001.

598 Ali, M., Fiori, A., and Bellotti, G.: Analysis of the nonlinear storage-discharge relation for hillslopes through 2D
599 numerical modelling, Hydrol. Process., 27, 2683-2690, https://doi.org/10.1002/hyp.9397, 2013.

600 Angermann, L., Jackish, C., Allroggen, N., Sprenger, M., Zehe, E., Tronicke, J., Weiler, M., and Blume, T.: Form
601 and function in hillslope hydrology: characterization of subsurface flow based on response observations,
602 Hydrolo. Earth Syst. Sci., 21, 3727-3748, https://doi.org/10.5194/hess-21-3727-2017, 2017.

603 Bachmair, S., and Weiler, M.: Hillslope characteristics as controls of subsurface flow variability, Hydrolo. Earth
604 Syst. Sci. 16, 3699-3715, https://doi.org/10.5194/hess-16-3699-2012, 2012.

605 Bachmair, S., Weiler, M., and Troch, P. A.: Intercomparing hillslope hydrological dynamics: Spatio-temporal
606 variability and vegetation cover effects, Water Resour. Res., 48, W05537, https://doi.org/
607 10.1029/2011WR011196, 2012.

608 Baroni, G., Ortuani, B., Facchi, A., and Gandolfi, C.: The role of vegetation and soil properties on the spatio-
609 temporal variability of the surface soil moisture in a maize-cropped field, J. Hydrol., 489, 148-159,
610 https://doi.org/10.1016/j.jhydrol.2013.03.007, 2013.

611 Beven, K. J., and Germann, P.: Macropores and water flow in soils, Water Resour. Res., 18, 1311-1325,
612 https://doi.org/10.1029/WR018i005p01311, 1982.

613 Beven, K., and Kirkby, M. J.: A physically based variable contributing area model of basin hydrology, Hydrol. Sci.
614 J., 24, 43-69, https://doi.org/10.1080/02626667909491834, 1979.

615 Brocca, L., Melone, F., Moramarco, T., and Morbidelli, R.: Spatial-temporal variability of soil moisture and it
616 estimation across scales, Water. Resour. Res., 46, W02516, https://doi.org/10.1029/2009WR008016, 2010.

617 Curtu, R., Mantilla, R., Fonley, M., Cunha, L. K., Small, S. J., Jay, L. O., and Krajewski, W. F.: An integral-balance
618 nonlinear model to simulate changes in soil moisture, groundwater and surface runoff dynamics at the
619 hillslope scale, Adv. Water Resour., 71, 125-139, https://doi.org/10.1016/j.advwatres.2014.06.003, 2014.

620 Farsadnia, F., Kamrood, M. R., Nia, A. M., Modarres, R., Bray, M. T., Han, D., and Sadatinejad, J.: Identification of
621 homogeneous regions for regionalization of watersheds by two-level self-organizing feature maps, J.
622 Hydrol., 509, 387-397, https://doi.org/10.1016/j.jhydrol.2013.11.050, 2014.

623 Feng, H., and Liu, Y.: Combined effects of precipitation and air temperature on soil moisture in different land covers
624 in a humid basin, J. Hydrol., 531, 1129-1140, https://doi.org/10.1016/j.jhydrol.2015.11.016, 2015.

625 Freer, J., McDonnell, J., Beven, K., Peters, N. E., Burns, D. A., Hooper, R. P., Aulenbach, B., and Kendall, C.: The
626 role of bedrock topography on subsurface storm flow, Water Resour. Res., 38(12), W1269, https://doi.org/
627 10.1029/2001WR000872, 2004,

628 Gao, L., and Shao, M.: Temporal stability of soil water storage in diverse soil layers, Catena, 95, 24-32,
629 https://doi.org/10.1016/j.catena.2012.02.020, 2012.

630 Gao, L., Shao, M., Xinhua, P., and She, D.: Spatio-temporal variability and temporal stability of water contents
631 distributed within soil profiles at a hillslope scale, Catena, 132, 29-36,
632 https://doi.org/10.1016/j.catena.2015.03.022, 2015.

633 Haga, H., Matsumoto, Y., Matsutani, J., Fujita, M., Nishida, K., and Sakamoto, Y.: Flow paths, rainfall properties,
634 and antecedent soil moisture controlling lags to peak discharge in a granitic unchanneled catchment, Water
635 Resour. Res., 41, W12410, https://doi.org/10.1029/2005WR004236, 2005.

636 He, Z., Zhao, W., Liu, H., and Chang, X.: The response of soil moisture to rainfall event size in subalpine grassland
637 and meadows in a semi-arid mountain range: a case study in northwestern China's Qilian Mountains, J.
638 Hydrol., 420-421, 183-190, https://doi.org/10.1016/j.jhydrol.2011.11.056, 2012.

639 Heisler-White, J. L., Knapp, A. K., and Kelly, E. F.: Increasing precipitation event size increases aboveground net
640 primary productivity in a semi-arid grassland, Oecologia, 158, 129-140, https://doi.org/10.1007/s00442-
641 008-1116-9, 2008.

642 Iglesias, F., and Kastner, W.: Analysis of similarity measures in times series clustering for the discovery of building
643 energy patterns, Energies, 6, 579-597, https://doi.org/10.3390/en6020579, 2013.

644 Kim, S.: Characterization of soil moisture responses on a hillslope to sequential rainfall events during late autumn
645 and spring, Water Resour. Res. 45, W09425, https://doi.org/ 10.1029/2008WR007239, 2009.

646 Kim, S.: Time series modeling of soil moisture dynamics on a steep mountainous hillside, J. Hydrol., 536, 37-49,
647 https://doi.org/ 10.1016/j.jhydrol.2016.02.027, 2016.

648 Kohonen, T.: Self-Organizing Maps, third ed., Springer, Berlin, 2001.

649 Lai, X., Liao, K., Feng, H., and, Zhu, Q.: Responses of soil water percolation to dynamic interactions among
650 rainfall, antecedent moisture and season in forest site, J. Hydrol., 540, 565-573,
651 https://doi.org/10.1016/j.jhydrol.2016.06.038, 2016.

652 Lee, E., and Kim, S.: Pattern Similarity Based Soil Moisture Analysis for Three Seasons on a Steep Hillslope, J.
653 Hydrol., 551, 484-494, https://doi.org/ 10.1016/jhydrol.2017.06.028, 2017

654 Ley, R., Casper, M. C., Hellebrand, H., and Merz, R.: Catchment classification by runoff behavior with self-
655 organizing maps (SOM), Hydrol. Earth Syst. Sci., 15, 2947-2962, https://doi.org/10.5194/hess-15-2947-
656 2011, 2011.

657 Li, X. Y., Zhang, S. Y., Peng, H. Y., Hu, X., and Ma, Y. J.: Soil water and temperature dynamics in shrub-
658 encroached grasslands and climatic implications: Results from inner Mongolia steppe ecosystem of north
659 China, Agric.For.Meteorol., 171, 20-30, https://doi.org/10.1016/j.agriformet.2012.11.001, 2013.

660 Liang, W. L., Kosugi, K., and Mizuyama, T.: Soil water dynamics around a tree on a hillslope with or without
661 rainwater supplied by stemflow, Water Resour. Res., 47, W02541, https://doi.org/10.1029/2010WR009856,
662 2011.

663 Liu, Y., Lee, S. H., and Chen, T. S.: Analysis of behavioral changes of zebrafish(Danio rerio) in response to
664 formaldehyde using Self-organizing map and a hidden Markov model, Ecol. Model., 222, 2191-2201,
665 https://doi.org/10.1016/j.ecolmodel.2011.02.010, 2011.

666 Liu, H., Lei, T. W., Zhao, J., Yuan, C. P., Fan, Y. T., and Qu, L. Q.: Effects of rainfall intensity and antecedent soil
667 water content on soil infiltrability under rainfall conditions using the runoff on out method, J. Hydrol., 396,
668 24-32, https://doi.org/10.1016/j.jhydrol.2010.10.028, 2011.

669 Minet, J., Verhoest, N. E. C., Lambot, S., and Vanclooster, M.: Temporal stability of soil moisture patterns
670 measured by proximal ground-penetrating radar, Hydrol. Earth Syst. Sci. Discuss., 10, 4063-4097,
671 http://doi.org/10.5194/hessd:10-4063-2013, 2013.

672 López García, H., and Machón González, I.: Self-organizing map and clustering for wastewater treatment
673 monitoring, Engineering Application of Artificial Intelligence, 17, 215-225, 2004.

674 Lu, N., and Godt, J.: Infinite slope stability under steady unsaturated seepage conditions, Water Resour. Res.,
675 W11404, https://doi.org/10.1029/2008WR006976, 2008.

676 Montero, P., and Vilar, J. A.: TSclust: An R package for time series clustering. J. Stat. Soft., 62(1), 1-43, 2014.

677 Park, Y. S., Cereghino, R., Compin, A., and Lek, S.: Applications of artificial neural networks for pattering and
678 predicting aquatic insect species richness in running waters, Ecol Model., 160, 265-280,
679 https://doi.org/10.1016/S0304-3800(02)00258-2, 2003.

680 Penna, D., Borga, M., Norbiato, D., and Fontana, G. D.: Hillslope scale soil moisture variability in a steep alpine
681 terrain, J. Hydrol., 364, 311-327, https://doi.org/10.1016/j.jhydrol.2008.11.009, 2009.

682 Penna, D., Tromp van Meerveld, H. J., Gobbi, A., Borga, M., and Fontana, G. D.: The influence of soil moisture on
683 threshold runoff generation processes in an alpine headwater catchment, Hydrol. Earth Syst. Sci., 15, 689-
684 702, https://doi.org/10.5194/hess-15-689-2011, 2011.

685 Penna, D., Brocca, L., Borga, M., and Fontana, G. D.: Soil moisture temporal stability at different depths on two
686 alpine hillslopes during wet and dry periods, J. Hydrol. 477, 55-71,
687 https://doi.org/10.1016/j.jhydrol.2012.10.052, 2013.

688 Ramirez, D. A., Bellot, J., Domingo, F., and Blasco, A.: Can water responses in stipa tenacissima L. during the
689 summer season be promoted by non-rainfall water gains in soil?, Plant and Soil, 291, 67-79,
690 https://doi.org/10.1007/s11104-006-9175-3, 2007.

691 Ran, Y., Li, X., Jin, R., Kang, J., and Cosh, M. H.: Strengths and weaknesses of temporal stability analysis for
692 monitoring and estimating grid-mean soil moisture in high-intensity irrigated agricultural landscape, Water
693 Resour. Res., 53, 283-301, https://doi.org/10.1002/2015WR018182, 2017.

694 Rodriguez-Iturbe, I., Isham, V., Cox, D. R., Manfreda, S., and Porporato, A.: Space-time modeling of soil moisture:
695 Stochastic rainfall forcing with heterogeneous vegetations, Water Resour. Res., 42, W06D05,
696 https://doi.org/10.1029/2005WR004497, 2006.

697 Rosenbaum, U., Bogena, H. R., Herbst, M., Huisman, J. A., Peterson, T. J., Weuthen, A., Western, A. W., and
698 Vereecken, H.: Seasonal and event dynamics of spatial soil moisture patterns at the small catchment scale,
699 Water Resour. Res., 48, W10544, https://doi.org/10.1029/2011WR011518, 2012.

700 Srivastava, P. K., Han, D., Ramirez, M. R., and Islam, T.: Machine learning techniques for downscaling SMOS
701 satellite soil moisture using MODIS land surface temperature for hydrological application, Water Resour.
702 Man., 27, 3127-3144, https://doi.org/10.1007/s11269-013-0337-9, 2013.

703 Tromp van Meerveld, I., and McDonnell, J.J.: Comment to "Spatial correlation of soil moisture in small catchments
704 and its relationship to dominant spatial hydrological processes, J.Hydrol., 286, 113-134", J.Hydrol., 303,
705 307-312, https://doi.org/10.1016/j.jhydrol.2004.09.002, 2005.

706 Uchida, T., Kosugi, K., and Mizuyama, T.: Effects of pipeflow on hydrological process and its relations to landslide,
707 a review of pipeflow studies in forested headwater catchments, Hydrol. Process. 15, 2151-2174,
708 https://doi.org/10.1002/hyp.281, 2001.

709 Vachaud, G., Passerat de Silans, A., Balabanis, P., and Vauclin, M.: Temporal stability of spatially measured soil
710 water probability density function, Soil Sci. Soc. Am. J., 49, 822-828,
711 https://doi.org/10.2136/sssaj1985.03615995004900040006x, 1985.

712 Van Arkel, Z., and Kaleita, A. L.: Identifying sampling locations for field-scale soil moisture estimation using K-
713 means clustering. Water Resour. Res. 50 (8), 7050-7057, https:/doi.org/10.1002/2013WR015015, 2014.

714 Wang, X. P., Cui, Y., Pan, Y. X., Li, X. R., Yu, Z., and Young, M. H.: Effects of rainfall characteristics on
715 infiltration and redistribution patterns in revegetation-stabilized desert ecosystems, J. Hydrol., 358, 134-
716 143, https://doi.org/10.1016/j,jhydrol.2008.06.002, 2008.

717 Wang, S., Fu, B., Gao, G., Liu, Y., and Zhou, J.: Responses of soil moisture in different land cover types to rainfall
718 events in a re-vegetation catchment area of the Loess Plateau, China, Catena, 101,122-128,
719 https://doi.org/10.1016/j,catena.2012.10.006, 2013.

720 Wienhöfer, J., and Zehe, E.: Predicting ssubsurface stormflow response of a forested hillslope: the role of connected
721 flow paths and bedrock topography, Hydrol. Earth Syst. Sci. Discuss., 10, 6473-6514,
722 http://doi.org/10.5194/hessd-10-6473-2013, 2013.

723 Wilson, D. J., Western, A. W., and Grayson, R. B.: Identifying and quantifying sources of variability in temporal
724 and spatial soil moisture observations, Water Resour. Res., 40, W02507,
725 https://doi.org/10.1029/2003WR002306, 2004.

726 Zhu, Q., Nie, X. F., Zhou, X. B., Liao, K. H., and Li, H. P.: Soil moisture response to rainfall at different
727 topographic positions along a mixed land-use hillslope, Catena, 119, 61-70,
728 https://doi.org/10.1016/j.catena.2014.03.010, 2014.

729 Zhao, Y., Peth, S., Wang, X. Y., Lin, H., and Horn, R.: Controls of surface soil moisture spatial patterns and their
730 temporal stability in a semi-arid steppe, Hydrol. Process, 24, 2507-2519, https://doi.org/10.1002/hyp.7665,
731 2010.
732
733
734
735
736

Hydrol. Earth Syst. Sci. Discuss., https://doi.org/10.5194/hess-2019-121
Manuscript under review for journal Hydrol. Earth Syst. Sci.
Discussion started: 3 April 2019

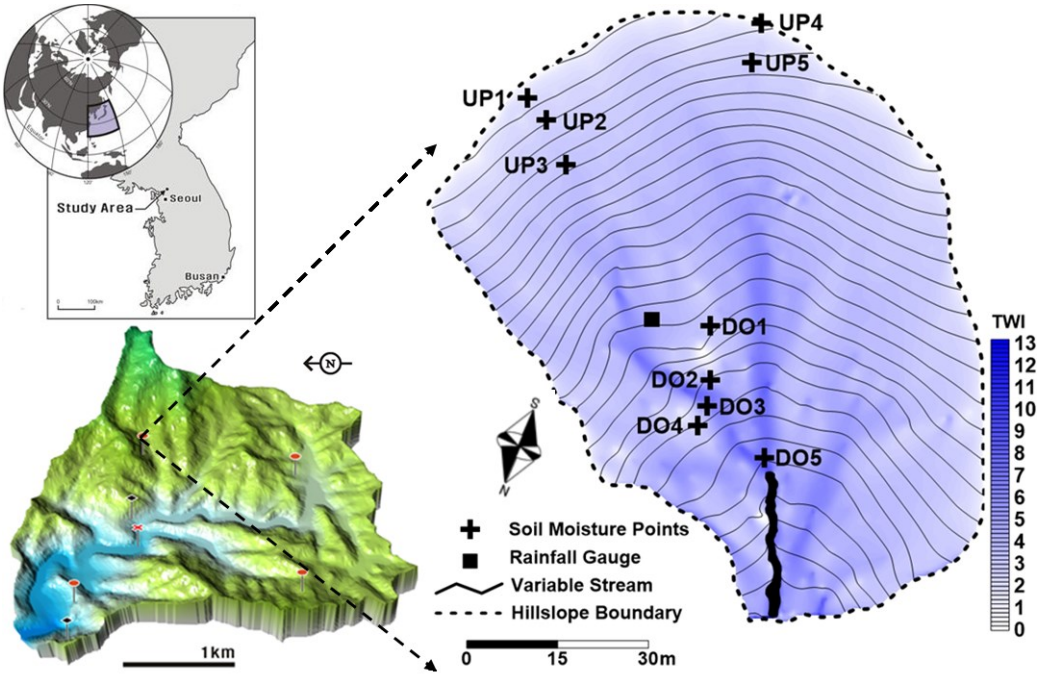

Figure 1. Location of the Sulmachun watershed in South Korea with hydrologic monitoring (rainfall and streamflow) stations (lower left) and study area with terrain contours, the topographic wetness index (TWI) (Beven and Kirkby, 1979), and soil moisture monitoring points (right).

Hydrol. Earth Syst. Sci. Discuss., https://doi.org/10.5194/hess-2019-121
Manuscript under review for journal Hydrol. Earth Syst. Sci.
Discussion started: 3 April 2019

Hydrology and Earth System Sciences
Discussions

750

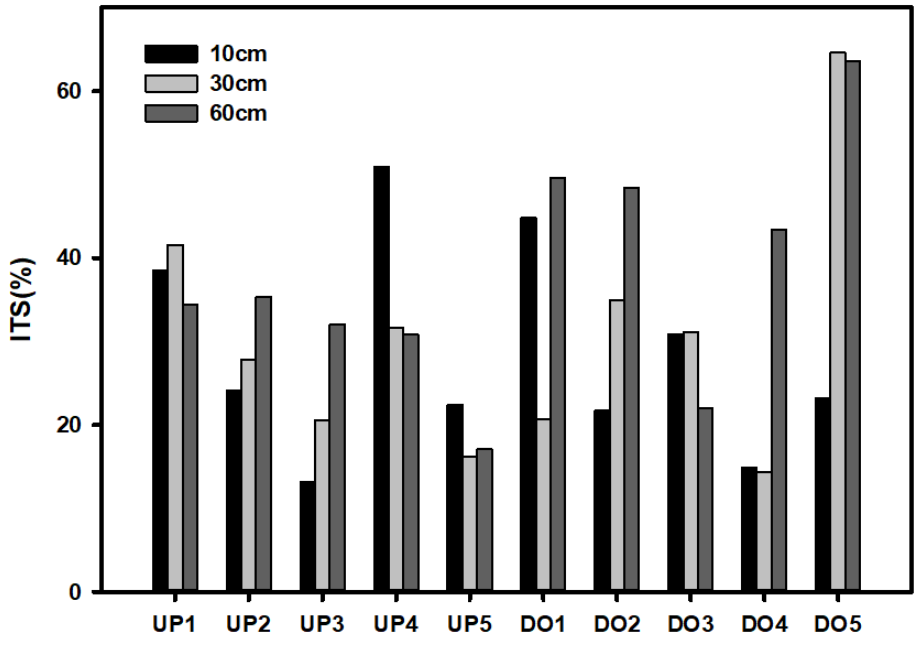

754 **Figure 2.** Indices of temporal stability (ITS) for 10 locations at depths of 10, 30, and 60 cm.

Hydrol. Earth Syst. Sci. Discuss., https://doi.org/10.5194/hess-2019-121
Manuscript under review for journal Hydrol. Earth Syst. Sci.
Discussion started: 3 April 2019

Hydrology and Earth System Sciences
Discussions

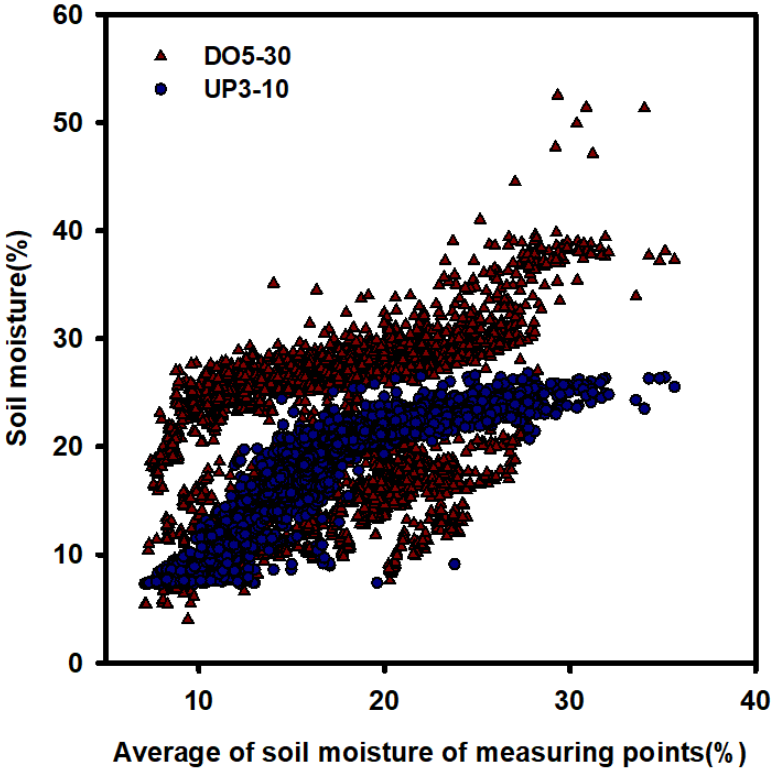

Figure 3. Soil moisture measurements for representative points (UP3-10) and the least temporally stable point (DO5-30) for the average soil moisture from 30 measurement points.

Hydrol. Earth Syst. Sci. Discuss., https://doi.org/10.5194/hess-2019-121
Manuscript under review for journal Hydrol. Earth Syst. Sci.
Discussion started: 3 April 2019

Hydrology and Earth System Sciences
Discussions

763

764

765

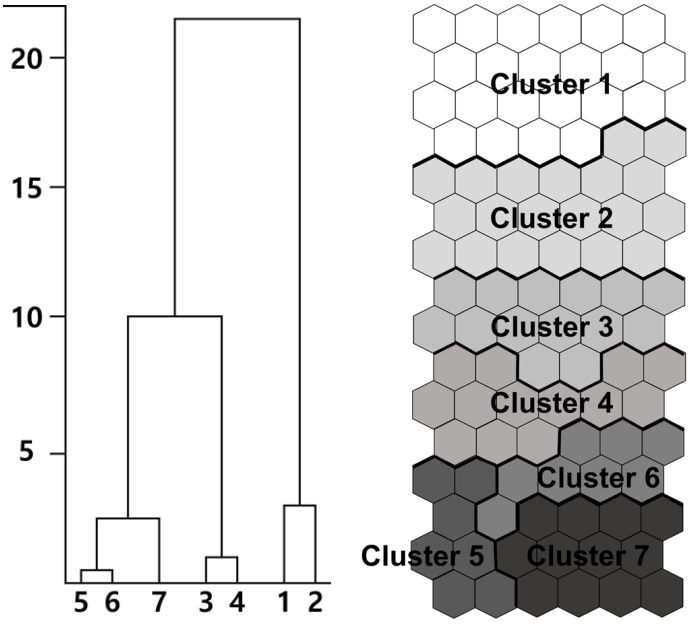

766

767 (a) (b)

768 **Figure 4.** Structure of the (**a**) dendrogram for seven clusters and (**b**) SOM classifications in 96 n

769 eurons through a 16 × 6 matrix.

770

771

772

773

Hydrol. Earth Syst. Sci. Discuss., https://doi.org/10.5194/hess-2019-121
Manuscript under review for journal Hydrol. Earth Syst. Sci.
Discussion started: 3 April 2019

Hydrology and Earth System Sciences
Discussions
Open Access
EGU

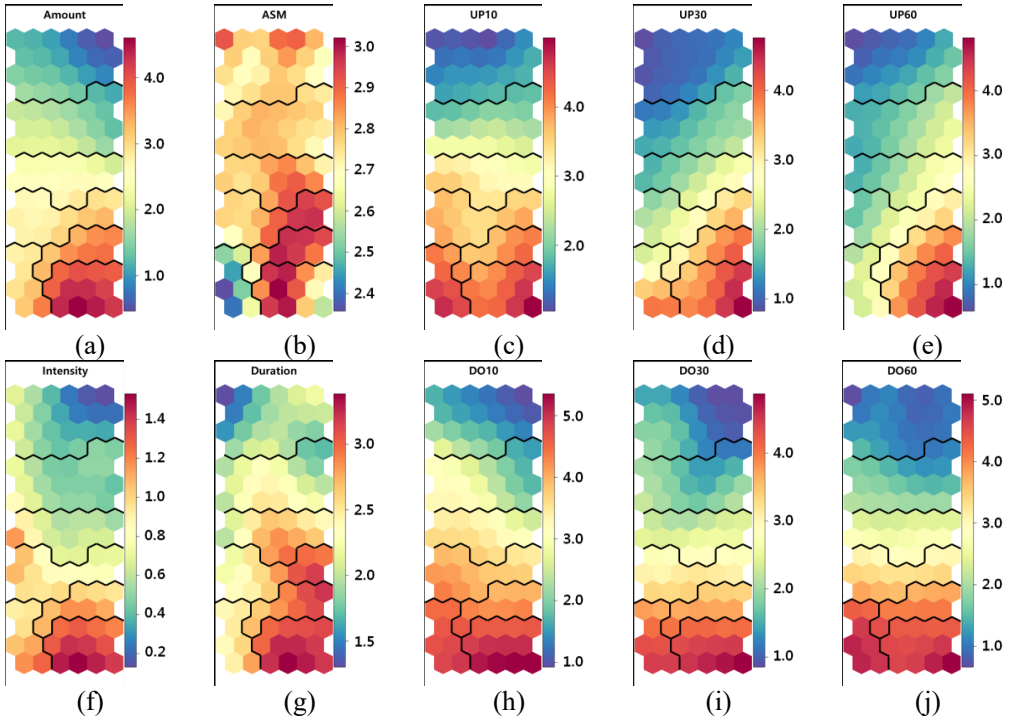

774 **Figures 5.** (**a**)–(**j**) Component planes of variable weightings for the rainfall amount, antecedent

775 soil moisture (ASM), soil moisture difference indices for the upslope at depths of 10, 30, and 60

Hydrol. Earth Syst. Sci. Discuss., https://doi.org/10.5194/hess-2019-121
Manuscript under review for journal Hydrol. Earth Syst. Sci.
Discussion started: 3 April 2019

776 cm, rainfall duration, rainfall intensity, and soil moisture difference indices for the downslope at
777 depths of 10, 30, and 60 cm.

778

779

Event projections of partial data SOM \ Event projections of complete data SOM	C1	C2	C3	C4	C5	C6	C7
C1	**127**	33					
C2		**34**	15				
C3		2	**26**	4			
C4			10	**24**	1	5	
C5					**24**	**1**	1
C6				5		19	
C7						2	**63**
Sum	127	69	51	33	25	27	64

780

781 **Figure 6.** 2D array expression of event projections for the summation of 10 SOMs of partial
782 datasets to the SOM of the complete dataset.

783

Hydrol. Earth Syst. Sci. Discuss., https://doi.org/10.5194/hess-2019-121
Manuscript under review for journal Hydrol. Earth Syst. Sci.
Discussion started: 3 April 2019

Hydrology and Earth System Sciences
Discussions

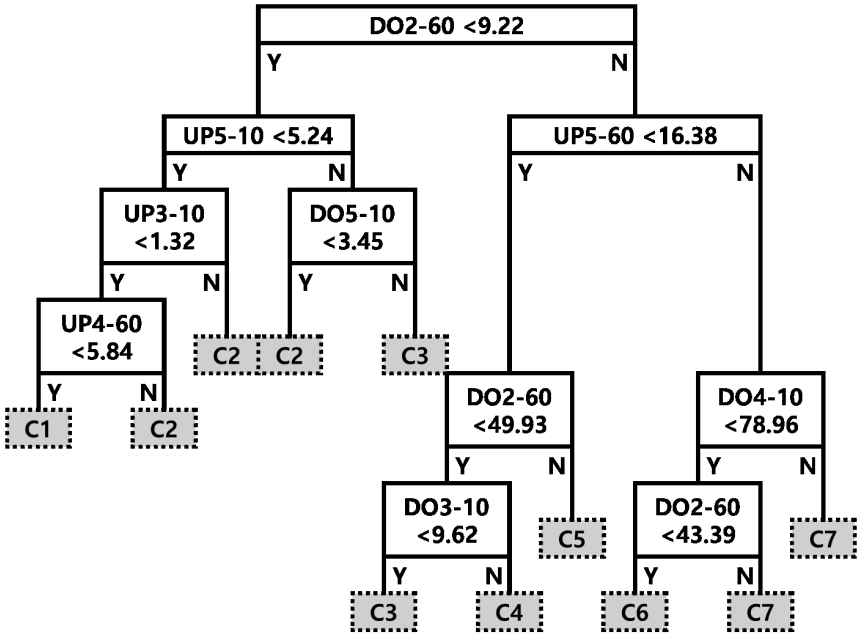

784

785 **Figure 7**. A C4.5 decision tree of soil moisture difference indices (numbers in boxes) for

786 hydrologic event classification.

Hydrol. Earth Syst. Sci. Discuss., https://doi.org/10.5194/hess-2019-121
Manuscript under review for journal Hydrol. Earth Syst. Sci.
Discussion started: 3 April 2019

787

788

789

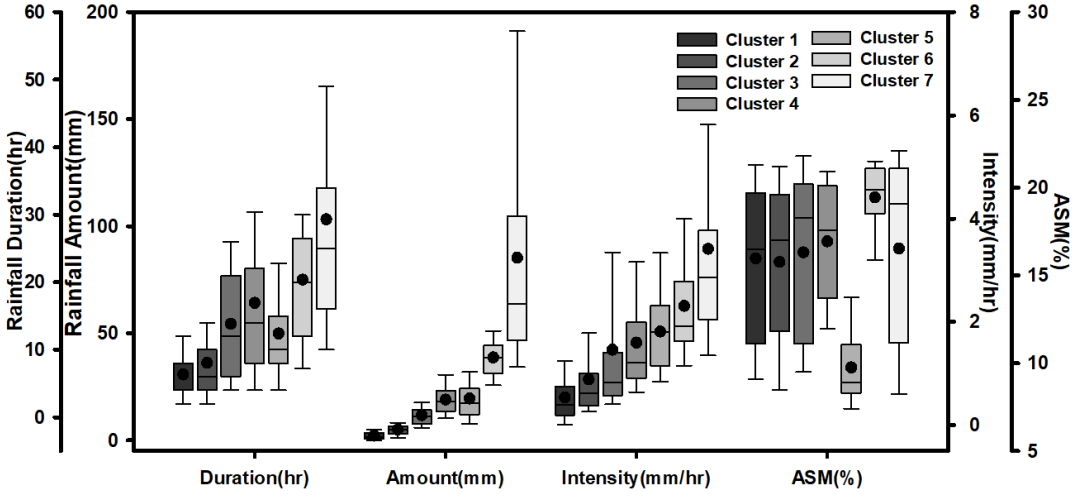

790

791 (a)

792

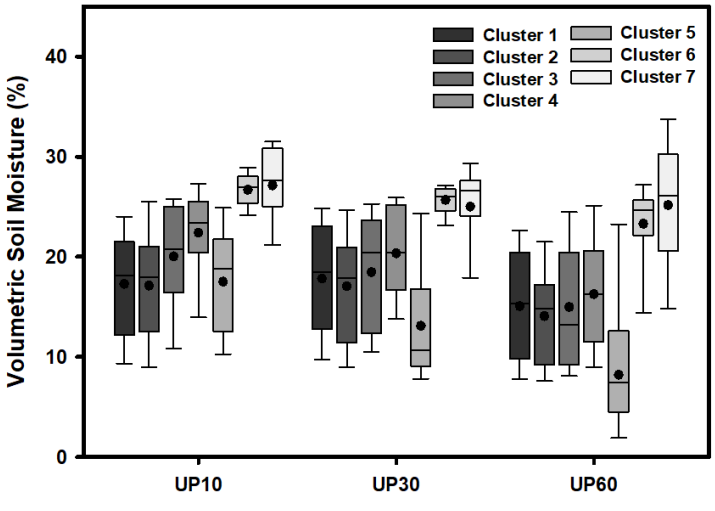

793

794 (b)

Hydrol. Earth Syst. Sci. Discuss., https://doi.org/10.5194/hess-2019-121
Manuscript under review for journal Hydrol. Earth Syst. Sci.
Discussion started: 3 April 2019

Hydrology and Earth System Sciences
Discussions

795

796

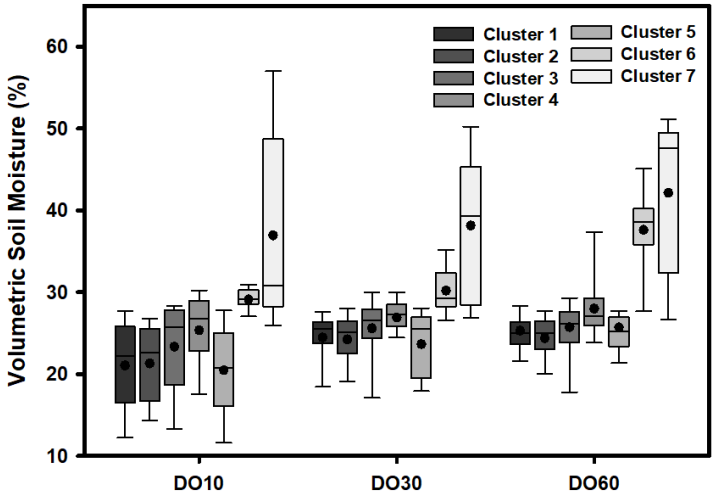

797

798 (c)

799 **Figure 8.** Statistical distributions of component vectors of (**a**) rainfall characteristics upslope, (**b**)

800 volumetric soil moisture, and (**c**) downslope volumetric soil moisture for the SOM classification.

801

802

803

804

805

806

807

808

809

810

Hydrol. Earth Syst. Sci. Discuss., https://doi.org/10.5194/hess-2019-121
Manuscript under review for journal Hydrol. Earth Syst. Sci.
Discussion started: 3 April 2019

811

812

813

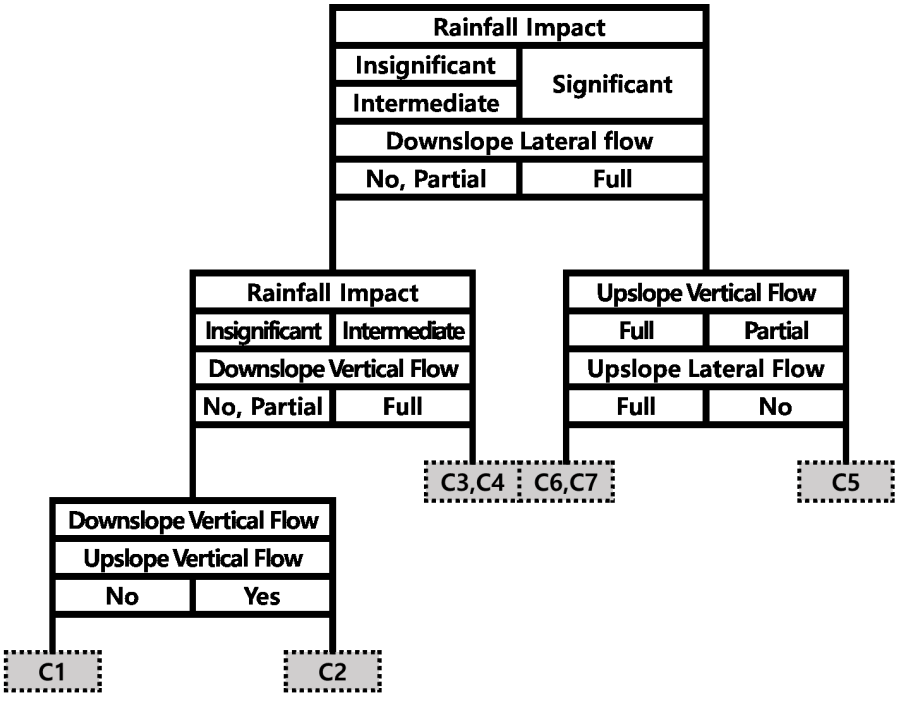

814

815 **Figure 9.** A decision tree of hydrological processes shown in Table 3; partial means that the
816 corresponding process was generated partially in the designated area; full indicates that the
817 hydrological process was generated at all depths and locations.

818

819

820

Hydrol. Earth Syst. Sci. Discuss., https://doi.org/10.5194/hess-2019-121
Manuscript under review for journal Hydrol. Earth Syst. Sci.
Discussion started: 3 April 2019

Hydrology and Earth System Sciences
Discussions

821

822 **Table 1.** Arithmetic averages of vector components for the rainfall duration (DUR), throughfall
823 amount (AMO), throughfall intensity (INT), antecedent soil moisture (ASM), means of the soil
824 moisture difference index at depths of 10, 30, and 60 cm for upslope points (UP10, UP30, and
825 UP60, respectively), and means of the soil moisture difference index at depths of 10, 30, and 60
826 cm for downslope points (DO10, DO30, and DO60, respectively).

Cluster	# of Event	DUR h	AMO mm	INT mm/h	ASM %	UP10 %	UP30 %	UP60 %	DO10 %	DO30 %	DO60 %
1	127	6.3	2.1	0.5	16.0	3.8	2.2	2.2	4.5	3.6	2.0
2	69	8.1	5.0	0.9	15.8	10.7	4.8	6.3	16.3	7.3	4.6
3	51	13.8	11.7	1.5	16.3	31.7	8.8	8.0	29.3	13.1	14.0
4	33	16.9	19.0	1.6	16.9	45.4	19.4	11.1	57.1	23.2	29.3
5	27	12.4	19.5	1.8	9.8	102.0	42.9	9.6	124.0	78.1	132.2
6	25	20.4	38.7	2.3	19.5	55.7	49.9	46.9	56.5	32.1	57.7
7	64	29.3	85.2	3.4	16.5	107.0	83.0	99.7	192.6	110.8	129.3

827

828

829

830

831

832

833

834

835

836

837

838

Hydrol. Earth Syst. Sci. Discuss., https://doi.org/10.5194/hess-2019-121
Manuscript under review for journal Hydrol. Earth Syst. Sci.
Discussion started: 3 April 2019

Hydrology and Earth System Sciences
Discussions

839 **Table 2.** Water storage analysis of selected rainfall events for all clusters.

Throughfall Impact		negligible		Intermediate		significant		
Year/Month		07/10	13/06	10/09	16/07	14/10	11/07	11/06
Cluster		1	2	3	4	5	6	7
Antecedent Soil Moisture		19.80	13.50	23.10	18.70	10.50	20.50	8.60
Throughfall (mm)		5.17	7.50	13.40	22.70	20.00	35.00	85.50
storage change (mm)	UP10	2.60	3.20	4.00	7.60	9.80	14.60	28.20
	UP30	1.40	0.80	3.60	4.80	1.00	11.00	26.40
	UP60	1.20	1.60	2.00	4.00	2.20	12.20	44.20
	DO10	3.60	2.20	12.40	12.40	20.80	16.40	37.00
	DO30	0.80	1.60	7.40	8.00	19.60	11.60	49.40
	DO60	1.50	3.60	25.50	15.90	47.10	40.20	116.10
soil moisture difference index (%)	UP10	4.50	6.67	11.56	35.05	55.63	58.33	184.21
	UP30	0.62	3.49	5.61	17.05	8.20	44.54	159.04
	UP60	0.91	3.85	2.90	13.46	5.41	35.98	306.94
	DO10	6.36	5.81	36.69	50.00	90.24	63.08	326.79
	DO30	0.97	5.43	13.17	14.77	88.99	24.43	261.70
	DO60	0.00	2.67	30.47	25.60	156.00	50.78	373.79

840

841

842

843

844

845

846

847

848

Hydrol. Earth Syst. Sci. Discuss., https://doi.org/10.5194/hess-2019-121
Manuscript under review for journal Hydrol. Earth Syst. Sci.
Discussion started: 3 April 2019

Hydrology and Earth System Sciences
Discussions

Table 3. Representative points of all clusters with coefficients of determination (R^2) and root mean square errors (RMSEs), and hydrological processes for all clusters.

Cluster		1	2	3	4	5	6	7
Representative Point		UP3-10	UP3-10	DO3-10	DO3-10	UP3-10	DO3-10	DO3-10
Statistics	R^2	0.919	0.943	0.946	0.805	0.637	0.721	0.806
	RMSE	1.547	1.705	1.851	1.880	2.110	1.568	3.132
rainfall impact		insignificant		Intermediate		Significant		
vertical flow	up slope	no	partial surface	full all	full all	partial middle	full all	full all
	down slope	no	partial surface	full all	full all	full all	full all	full all
lateral flow	up slope	no	no	no	No	no	full surface bedrock	full surface bedrock
	down slope	no	no	partial bedrock	partial bedrock	full surface bedrock	full surface bedrock	full surface bedrock

partial: the corresponding flowpath was generated partially in the designated part; full: the process was generated at all depths and locations; surface: the process was generated at a depth of 10 cm; middle: the process was generated up to a depth of 30 cm; all: the process was generated at all depths; bedrock: the process was generated at a depth of 60 cm.